Electronic Supplementary Information

An Unfused-Ring Acceptor with High Side-Chain Economy Enabling 11.17% As-Cast Organic Solar Cells

Fuqiang Du,[a] *Hongtao Wang,*[a,b] *Lingqiang Yang,*[a] *Jinru Cao,* [a] *Jiangsheng Yu*[b*] *and Weihua Tang*[*a]

[a] School of Chemical Engineering, Nanjing University of Science and Technology, Nanjing 210094, P.R. China.
E-mail: whtang@njust.edu.cn.

[b] MIIT Key Laboratory of Advanced Solid Laser, Nanjing University of Science and Technology, Nanjing 210094, P.R. China.
E-mail: yjs@njust.edu.cn.

Table of content

1. Experimental Section

1.1 Materials

All reagents and solvents, unless otherwise specified, were purchased from Energy

Chemical, Tansoole, J&K, energy chemical or Sigma-Aldrich and were used without further purification. Column chromatography was carried out with 300-400 nm mesh silica. The synthetic routes of DCB-4F and CB-4F are shown in **Scheme S1**.

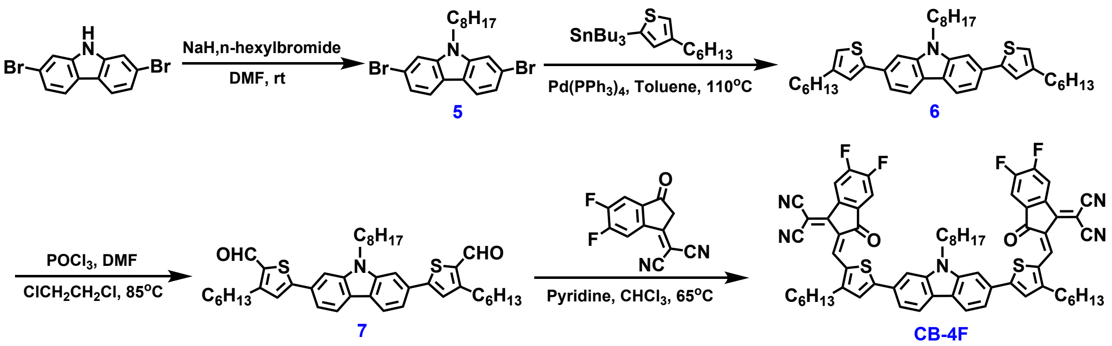

Scheme S1. Synthetic routes of CB-4F.

2,7-Dibromo-9-octyl-9H-carbazole **(5):** The synthesis of compound **5** was similar to 7-octyl-7H-dibenzo[c,g]carbazole. The residue was purified by silica gel column chromatography with petroleum ether to obtain a colorless oil (90% yield). ^{1}H NMR (500 MHz, CDCl3, δ): 7.89 (d, 2H), 7.53 (s, 2H), 7.34 (d, 2H), 4.19 (t, 2H), 1.88-1.80 (m, 2H), 1.42-1.21 (m, 10H), 0.88 (t, 3H). ^{13}C NMR (125 MHz, $CDCl_3$) δ 141.55, 122.71, 121.68, 121.46, 119.88, 112.20, 43.54, 31.98, 29.50, 29.37, 28.97, 27.37, 22.82, 14.29.

2,7-Bis(4-hexylthiophen-2-yl)-9-octyl-9H-carbazole **(6):** The synthesis of compound **6** was similar to 5,9-bis(4-hexylthiophen-2-yl)-7-octyl-7H-dibenzo[c,g]carbazole. The residue was purified by silica gel column chromatography with petroleum ether/dichloromethane (9:1, v/v) to obtain a colorless oil (86% yield). ^{1}H NMR (500 MHz, $CDCl_3$, δ):8.02 (d, 2H), 7.57 (s, 2H), 7.50 (d, 2H), 7.28 (s, 2H), 6.92 (s, 2H), 4.34 (t, 2H), 2.68 (t, 4H), 1.92 (m, 2H), 1.72 (m, 4H), 1.47-1.26 (m, 22H), 0.95 (m, 6H), 0.89 (m, 3H). ^{13}C NMR (125 MHz, $CDCl_3$, δ): 145.38, 144.55, 141.62, 132.60, 124.68, 122.30, 120.73, 119.44, 117.83, 105.91, 43.16, 32.05, 31.94, 30.94, 30.68, 29.55, 29.39, 29.29, 29.12, 27.43, 22.86, 22.84, 14.34, 14.29.

5,5'-(9-Octyl-9H-carbazole-2,7-diyl)bis(3-hexylthiophene-2-carbaldehyde) **(7):**

The synthesis of compound 7 was similar to 5,5'-(7-octyl-7H-dibenzo[c,g]carbazole-5,9-diyl)bis(3-hexylthiophene-2-carbaldehyde). The residue was purified by silica gel column chromatography with petroleum ether/dichloromethane (1:3, v/v) to obtain a yellow solid (76% yield). ^{1}H NMR (500 MHz, $CDCl_3$, δ): 10.01 (s, 2H), 7.97 (d, 2H), 7.54 (d, 2H), 7.47 (d, 2H), 7.27 (s, 2H), 4.22 (t, 2H), 2.94 (t, 4H), 1.91 - 1.78 (m, 2H), 1.77 - 1.64 (m, 4H), 1.49 - 1.11 (m, 22H), 1.00 – 0.75 (m, 9H). ^{13}C NMR (125 MHz, $CDCl_3$, δ): 181.80, 154.22, 154.15, 141.51, 136.44, 131.20, 126.50, 123.38, 121.14, 117.97, 106.53, 43.16, 31.93, 31.72, 31.62, 29.84, 29.44, 29.30, 29.20, 29.06, 28.81, 27.34, 22.74, 22.71, 14.21.

CB-4F: 2-(5-Fluoro-3-oxo-2,3-dihydro-1H-inden-1-ylidene) malononitrile (310.1mg, 0.135 mmol) was added into the solution of compound **7** (150mg, 224.6 μmol) in chloroform (15 mL) with pyridine (0.1 mL), the mixture was deoxygenated with nitrogen for 20 min and then refluxed for 4 h. After cooling to room temperature and removal of the solvent under vacuum, the residue was then washed with methanol and hexane. The dark solid was obtained without further purification (117.7 mg, 48% yield). ^{1}H NMR (500 MHz, $CDCl_3$, δ): 9.02 (s, 2H), 8.55 (d, 2H), 8.13 (d, 2H), 7.82 - 7.64 (m, 6H), 7.53 (s, 2H), 4.46 (s, 2H), 3.10 - 2.99 (m, 4H), 2.27 - 2.18 (m, 2H), 1.99 (d, 4H), 1.31 (d, 22H), 0.87 (m, 9H). ^{13}C NMR (175 MHz, pyridine-d5, δ): 204.57, 186.34, 185.51, 181.75, 174.89, 162.60, 159.96, 159.22, 154.73, 153.81, 142.35, 136.77, 131.95, 131.75, 130.01, 127.88, 124.54, 119.10, 115.20, 114.93, 114.47, 112.52, 107.69, 79.18, 78.99, 78.80, 43.19, 36.01, 31.67, 30.31, 29.67, 29.25, 28.64, 27.08, 25.85, 22.49, 13.82. MALDI-TOF MS: m/z = 1091.3888 $[M]^+$, calcd. for $C_{66}H_{57}N_5O_2S_2F_4$, 1091.3890.

1.2 Instruments and general methods

Most ^{1}H NMR and ^{13}C NMR spectra were recorded on Bruker AVANCE III (500 MHz) nuclear magnetic resonance (NMR) spectroscope with tetramethylsilane (TMS) as internal standard. Specifically, the ^{13}C NMR spectrum for CB-4F was collected on Bruker AVANCE NEO (700 MHz) NMR spectroscopy with TMS as standard. UV-vis absorption spectra were recorded on Evolution 220, Thermo Fisher spectrophotometer.

Thermogravimetric analysis (TGA) was conducted on TGA/SDTA851E (Mettler Toledo) under nitrogen atmosphere at a heating rate of 20 °C min^{-1} from 50 °C to 800 °C. The electrochemical Cyclic voltammetry (CV) measurements were carried out on an electrochemical workstation (CHI760D Chenhua, Shanghai) with Pt plate as working electrode, Pt slice as counter electrode, and Ag/AgCl electrode as reference electrode in tetrabutylammonium hexafluorophosphate (n-$\mathrm{Bu_4NPF_6}$, 0.1 M) dichloromethane solutions at a scan rate of 50 mV s^{-1}. The CV curves were recorded and calibrated by the ferrocene-ferrocenium (Fc/Fc+) redox couple (-4.8 eV versus vacuum level). The materials were measured by coating a film on the surface of working electrode. The HOMO and LUMO levels are calculated by the formula: $E_{HOMO} = -[E_{OX} + (4.8 - E_{FC/FC+})]$, $E_{LUMO} = -[E_{RED} + (4.8 - E_{FC/FC+})]$, where E_{OX}/E_{RED} means the potential from the first oxidation or reduction peak and $E_{Fc/Fc+}$ means the half-wave potential of the external standard.

1.3 Space-Charge Limited Current (SCLC) Measurement

The hole and electron mobility were measured using the space charge limited current (SCLC) method, employing a diode configuration of ITO/PEDOT:PSS/active layer/$\mathrm{MoO_3}$/Ag for hole and ITO/ZnO/active layer/PDINO/Al for electron, respectively. The charge mobility can be determined based on the Mott-Gurney equation with Poole-Frenkel correction:

$$J(\mathrm{V}) = \frac{9\mathrm{V}^2}{8\mathrm{L}^3}\varepsilon_0\varepsilon_r\mu_0 e^{\left(0.89\gamma\sqrt{\mathrm{V}/\mathrm{L}}\right)}$$

Here, ε_r is dielectric constant of organic materials, ε_0 is the free space permittivity, L is the thickness of active layer, μ_0 is the charge carrier mobility, and V is the applied voltage.

1.4 Solubility measurement

To 10 mL chloroform was added 50 mg DCB-4F or CB-4F. The solutions were sonicated at 25°C for 2 h. Then extra DCB-4F or CB-4F (25 mg) was added to the solution per hour until solid precipitate could be observed. For DCB-4F, two times addition was needed while CB-4F only needed once. After that, the solutions were centrifuged and the supernatant was used for solubility measurement. The solution (100 μL) was pipetted onto the hot petri dish. Then the film mass was weighed after the solvent was completely evaporated to calculate the solubility of two acceptors.

2. Comparison of as-cast OSCs' PCEs and sidechain weight ratio for best-performing UFAs

Table S1 Comparison of as-cast PCE and side chain weight ratio of the best-performing UFAs for high-performance OSCs in literature.

NFA	E_g^{opt} (eV)	HOMO/ LUMO (eV)	Donor	V_{oc} (V)	J_{sc} (mA cm^{-2})	FF (%)	As-cast PCE (%)	Sidechain (wt %)	Ref.
DCB-4F	**1.55**	**-5.50/-3.86**	**PM6**	**1.00**	**16.42**	**58.23**	**9.56**	**23.78**	**This work**
HC-PCIC	1.48	-5.54/-3.87	PTQ10	0.94	15.99	67.96	**4.35**	30.98	[1]
HC-PCIC	1.48	-5.54/-3.87	PM6	0.88	17.54	72.69	**6.29**	30.98	[1]
BT2F-IC4F	1.38	-5.98/-4.31	PBDB-T	0.67	19.43	64.7	**7.04**	31.15	[2]
BT-IC4F	1.37	-5.89/-4.27	PBDB-T	0.69	21.4	66.4	**7.85**	31.94	[2]
HF-PCIC	1.5	-5.53/-3.83	PM6	0.91	17.81	70.77	**9.23**	32.44	[1]
DF-PCIC	1.59	-5.49/-3.77	PBDB-T	0.91	15.66	72	**6.21**	34.21	[3]
BDTC-4Cl	1.42	-5.35/-3.75	PBDB-T	0.86	18.56	59.5	**5.57**	35.26	[4]
CTIC-4F	1.3	-5.4/-4.0	PTB7-Th	0.7	23.4	64	**8.68**	35.61	[5]
CO1-4F	1.2	-5.3/-4.1	PTB7-Th	0.64	24.8	64	**8.51**	36.41	[5]
COTIC-4F	1.1	-5.2/-4.1	PTB7-Th	0.57	20.7	61	**5.59**	37.19	[5]
X-PCIC	1.37	-5.37/-3.79	PBDB-T	0.84	21.8	62.51	**6.29**	37.95	[6]
X1-PCIC	1.39	-5.35/-3.77	PBDB-T	0.85	17.97	66.82	**6.64**	39.38	[6]
PTICH	1.6	-5.62/-3.80	PM6	0.92	8.22	54	**4.08**	40.12	[7]
NOC6F-1	1.58	-5.55/-3.77	PBDB-T	0.95	17.08	65.79	**10.62**	40.79	[8]
BTOR-IC4F	1.37	-5.92/-4.23	PBDB-T	0.8	20.57	69.6	**10.18**	42.48	[2]
Ph-IC	1.62	-5.72/-3.79	PBFTZ	0.89	12.37	51.5	**4.45**	42.67	[9]
DOC6-IC	1.43	-5.33/-3.72	PBDB-T	0.91	19.21	60.11	**8.72**	44.03	[10]
PTIC	1.53	-5.59/-3.81	PM6	0.93	16.73	66	**10.27**	47.61	[7]

PTICO	1.56	-5.48/-3.66	PM6	1.01	12.6	52	**6.62**	48.81	[7]

The chemical structures for the UFAs in **Table S1** are listed as below. The weight ratio of side chain is also calculated according to equation inside.

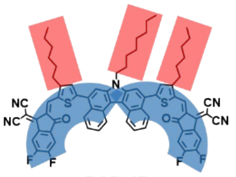

DCB-4F

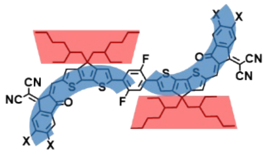

DF-PCIC, X=H
HC-PCIC, X=Cl

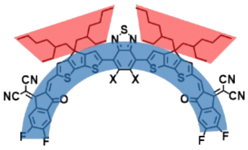

BT-IC4F, X=H
BT2F-IC4F, X=F

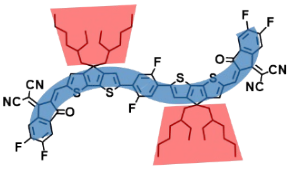

HF-PCIC

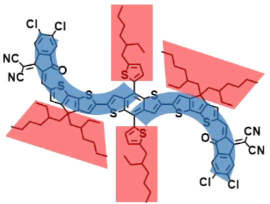

BDTC-4Cl

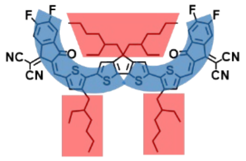

CTIC-4F

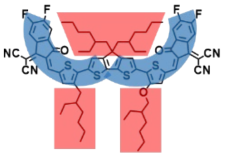

CO1-4F

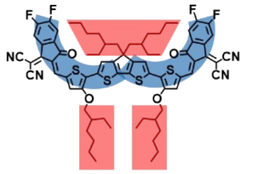

COTIC-4F

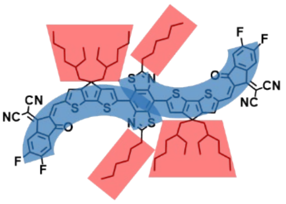

X-PCIC

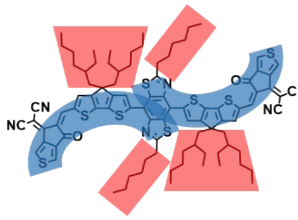

X1-PCIC

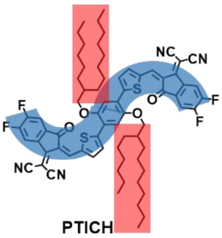

PTICH

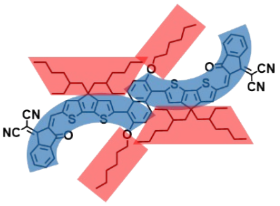

NOC6F-1

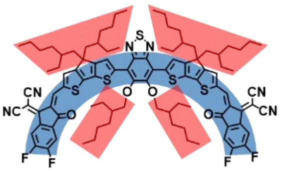

BTOR-IC4F

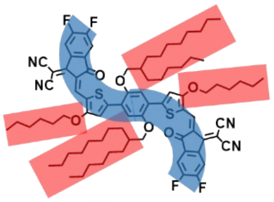

PTICO

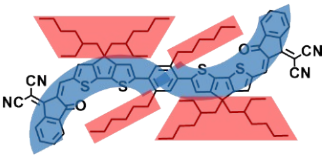

DOC6-IC

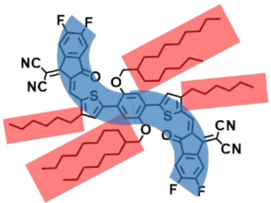

PTIC

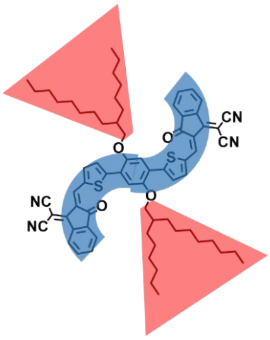

Ph-IC

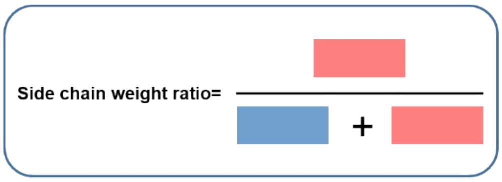

3. NMR and mass spectra

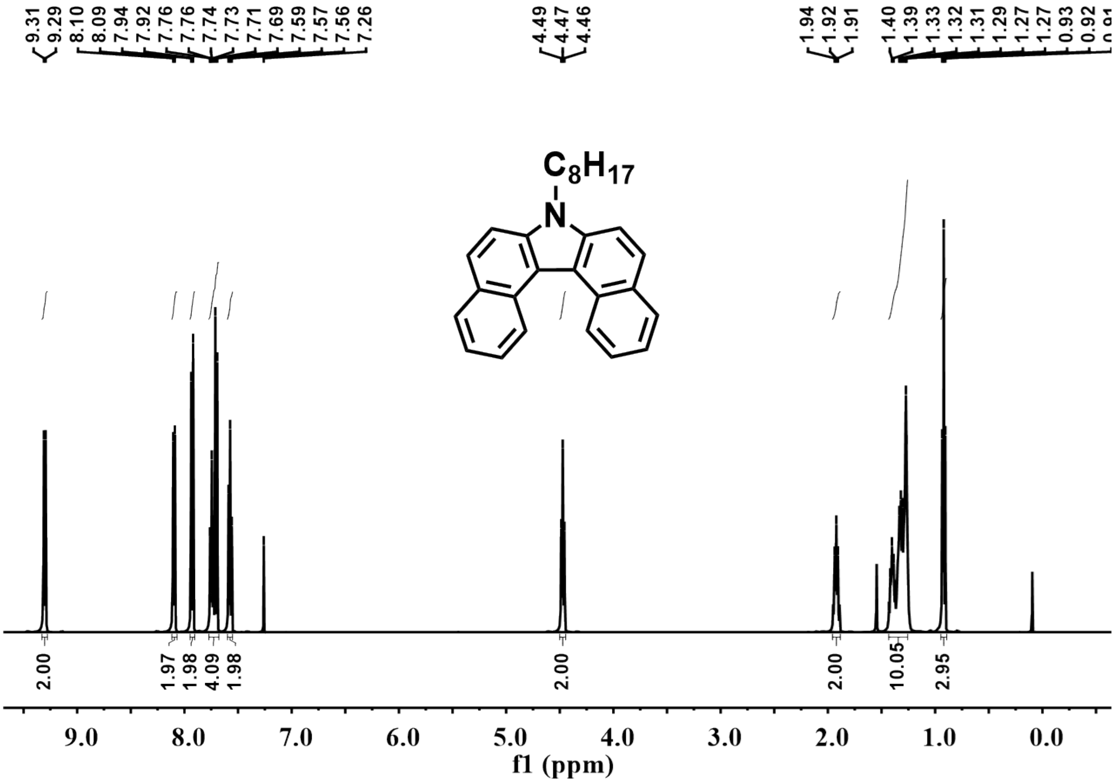

Fig. S1 ^{1}H NMR spectrum of **compound 1**.

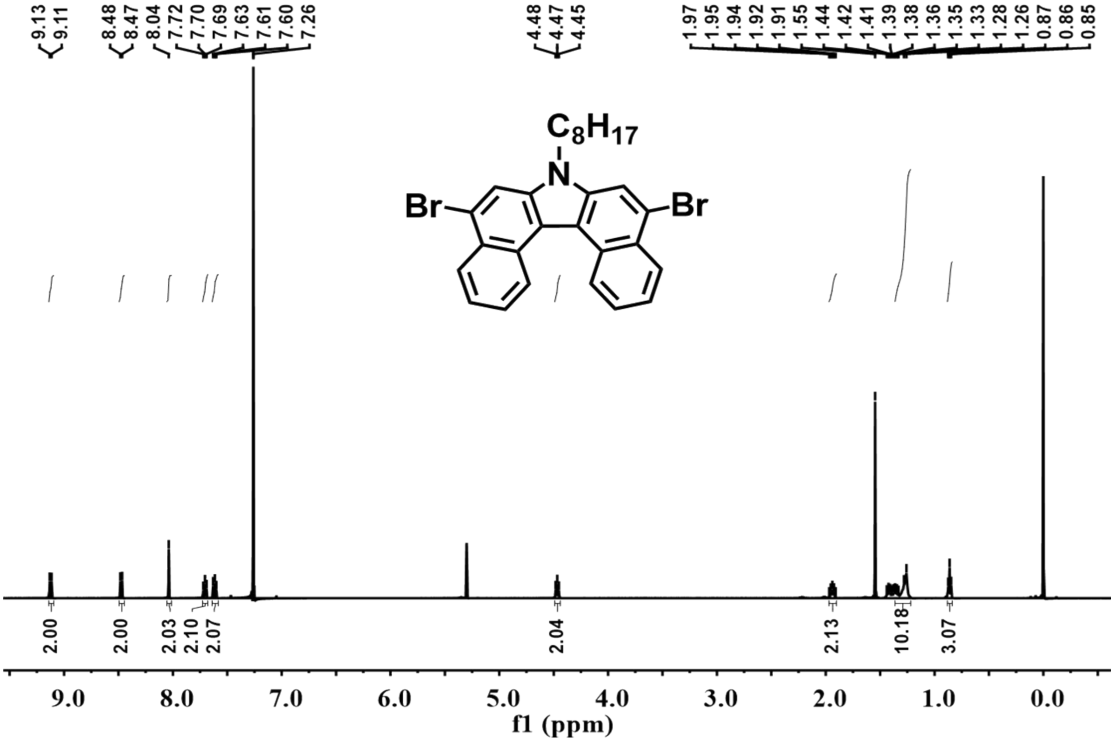

Fig. S2 ^{1}H NMR spectrum of **compound 2**.

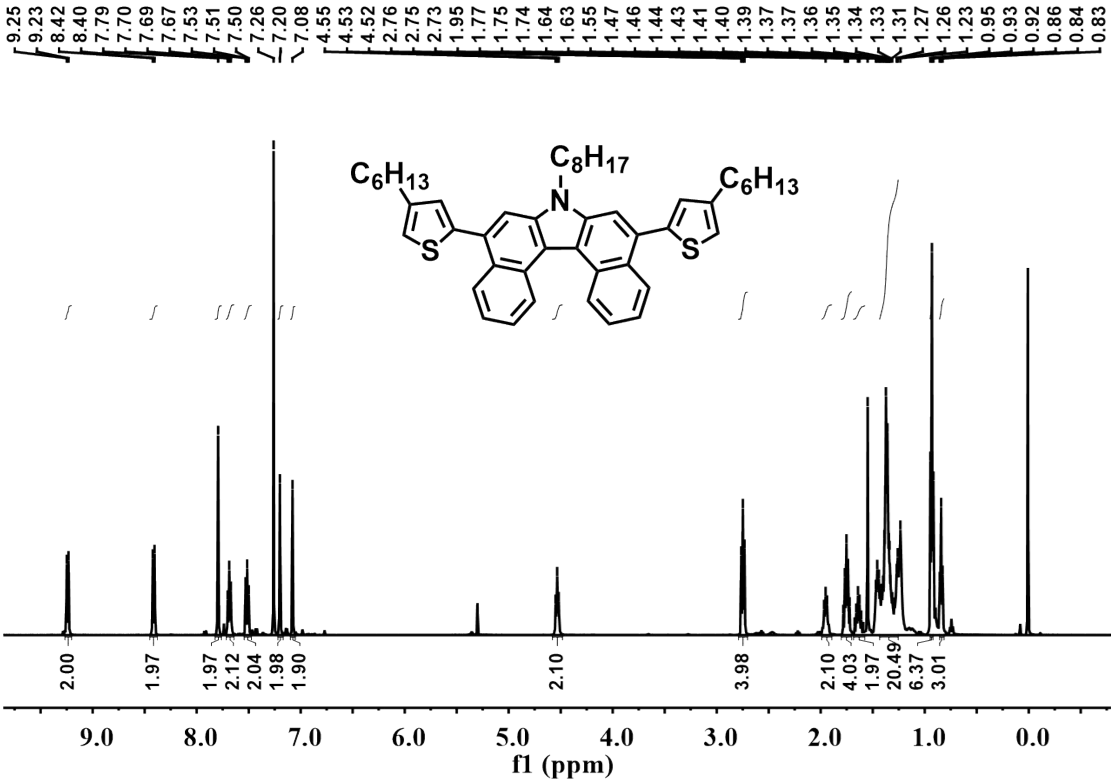

Fig. S3 ^{1}H NMR spectrum of **compound 3**.

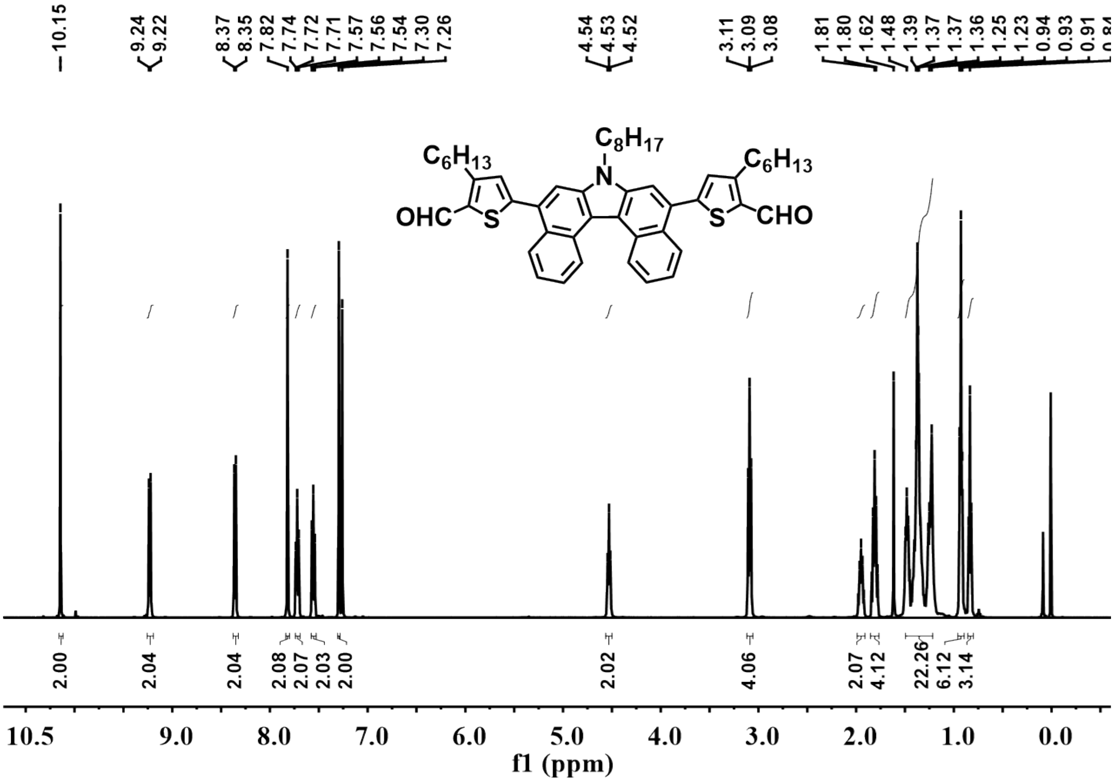

Fig. S4 ^{1}H NMR spectrum of **compound 4**.

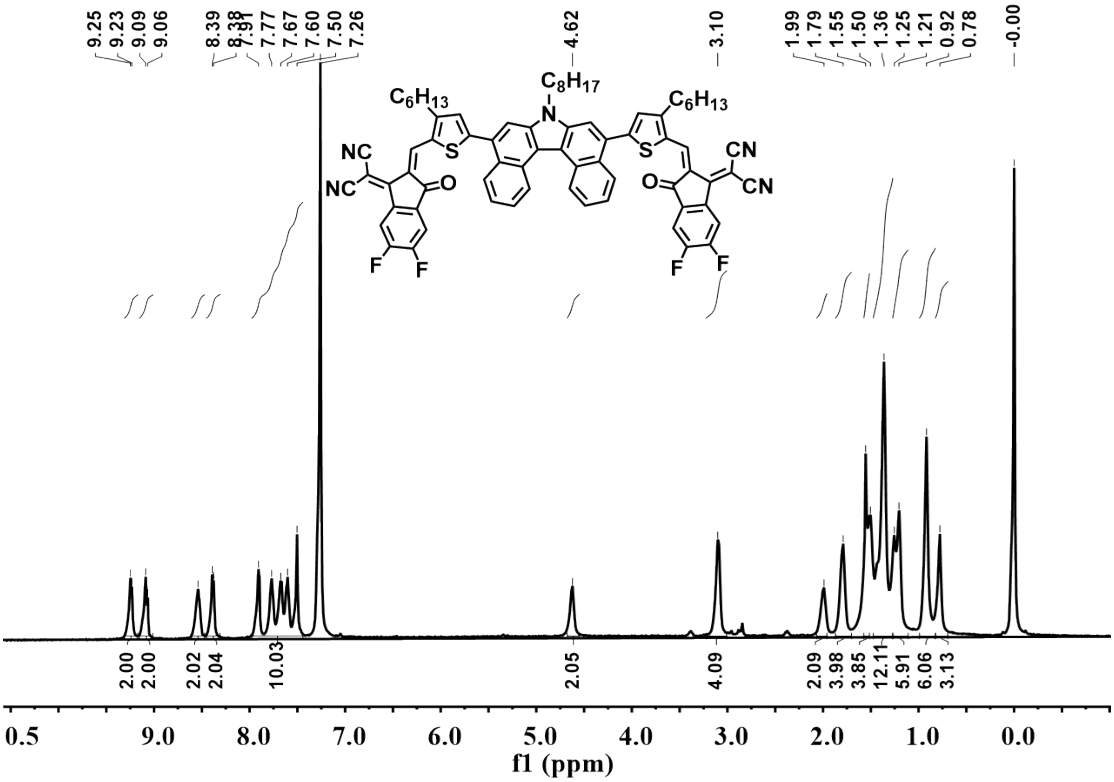

Fig. S5 ^{1}H NMR spectrum of **DCB-4F**.

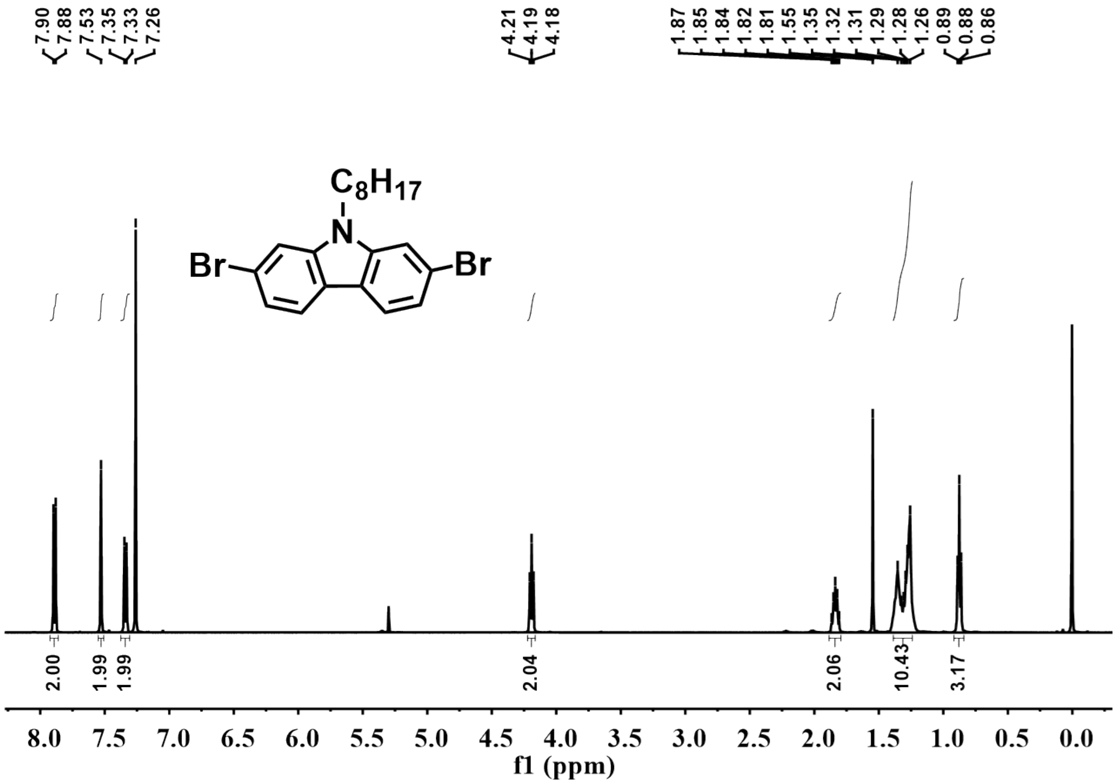

Fig. S6 ^{1}H NMR spectrum of **compound 5**.

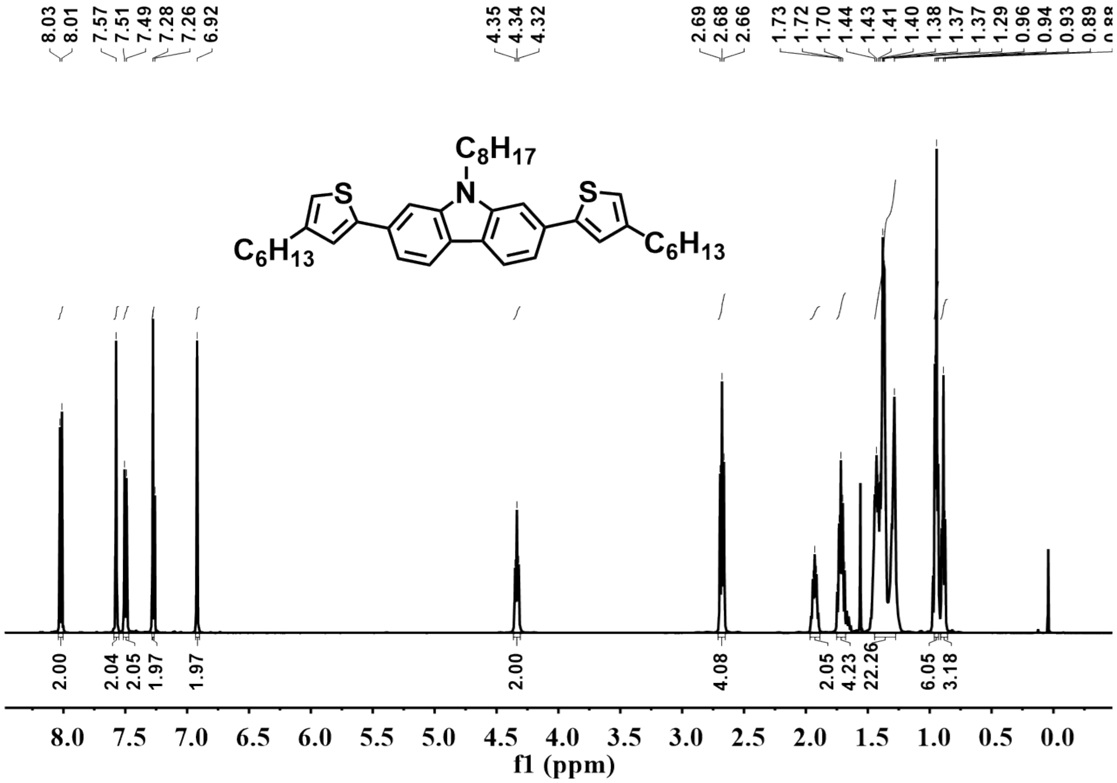

Fig. S7 ^{1}H NMR spectrum of **compound 6**.

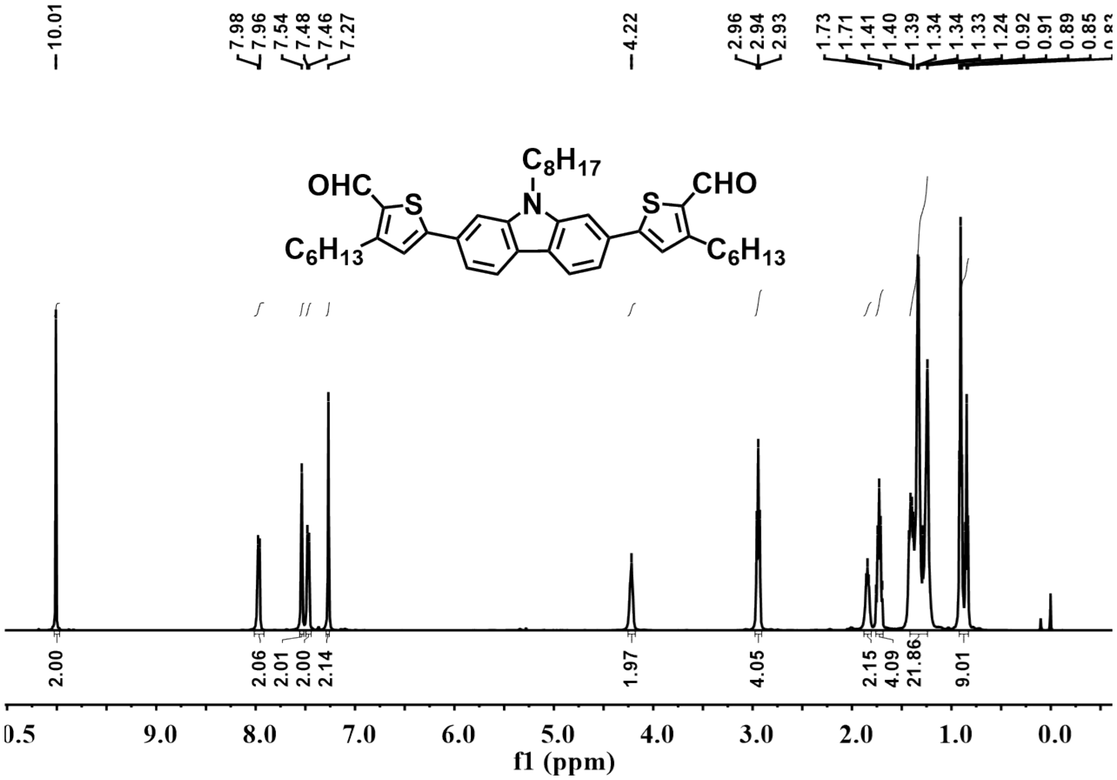

Fig. S8 ^{1}H NMR spectrum of **compound 7**.

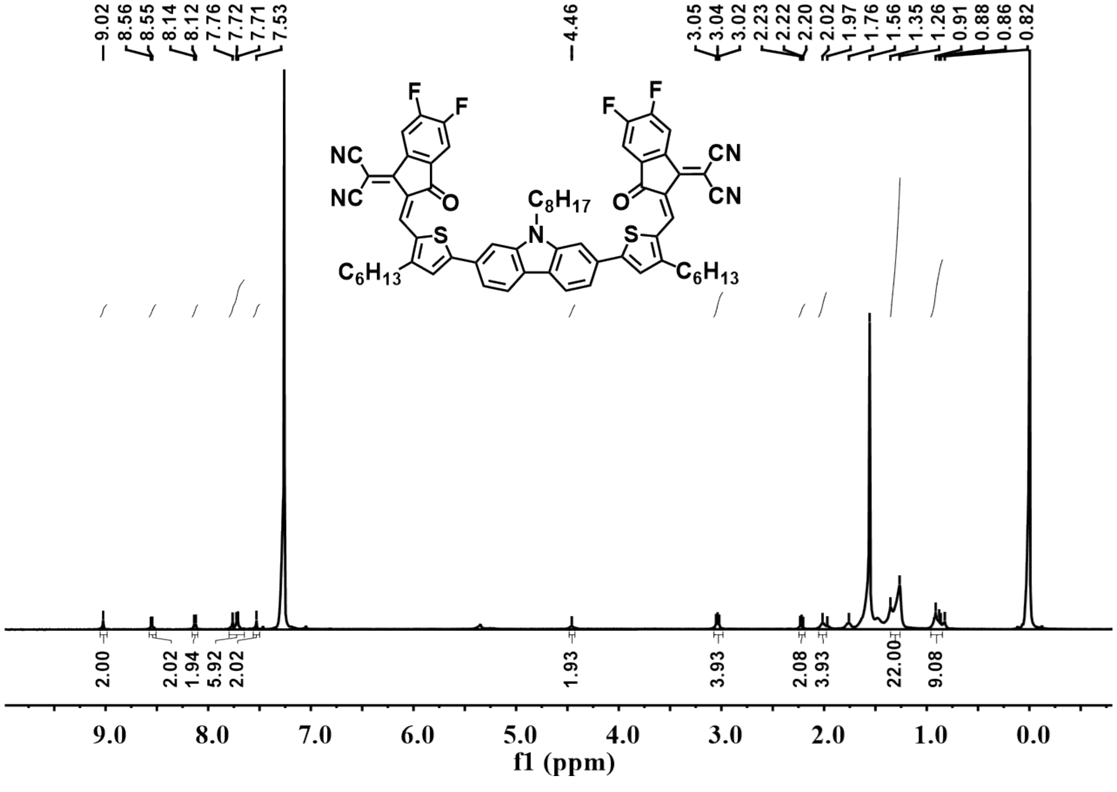

Fig. S9 ^{1}H NMR spectrum of **CB-4F**.

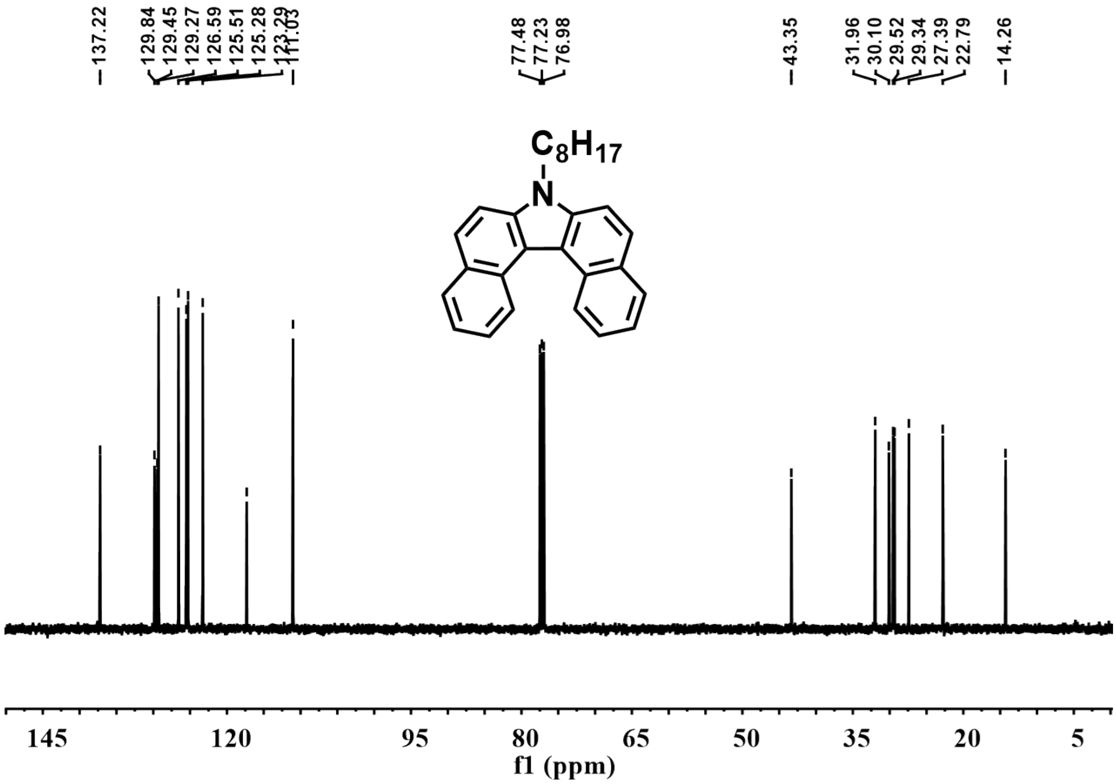

Fig. S10 ^{13}C NMR spectrum of **Compound 1**.

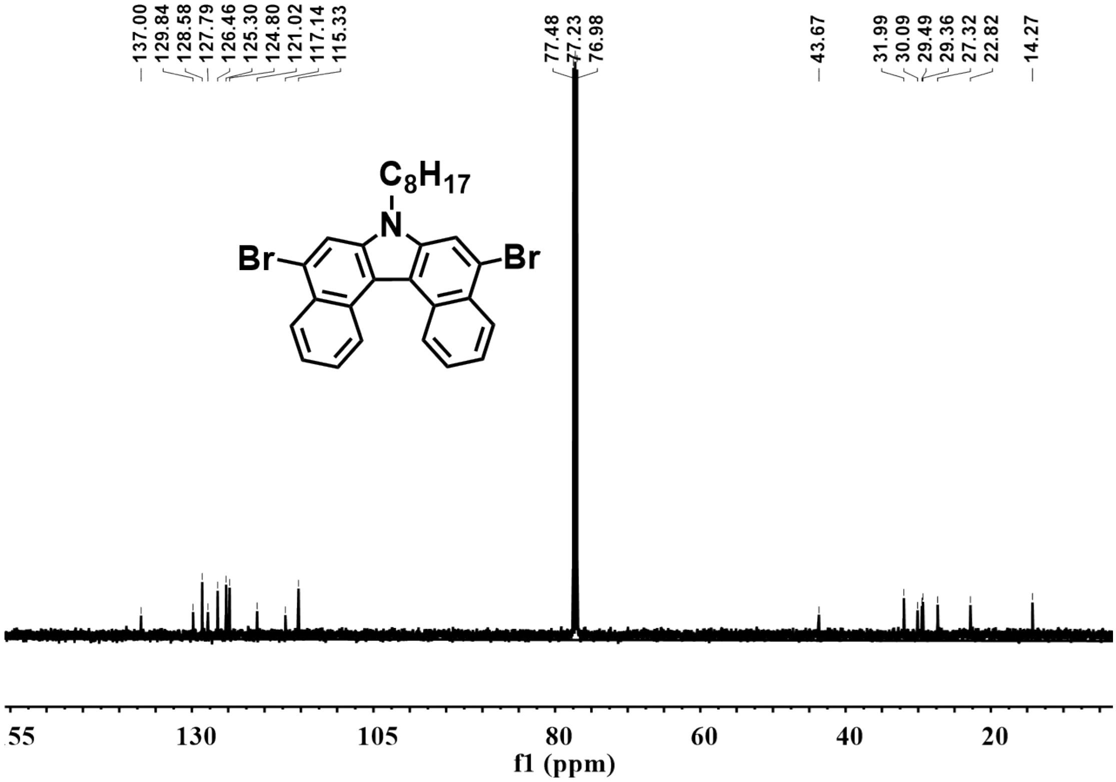

Fig. S11 ^{13}C NMR spectrum of **Compound 2**.

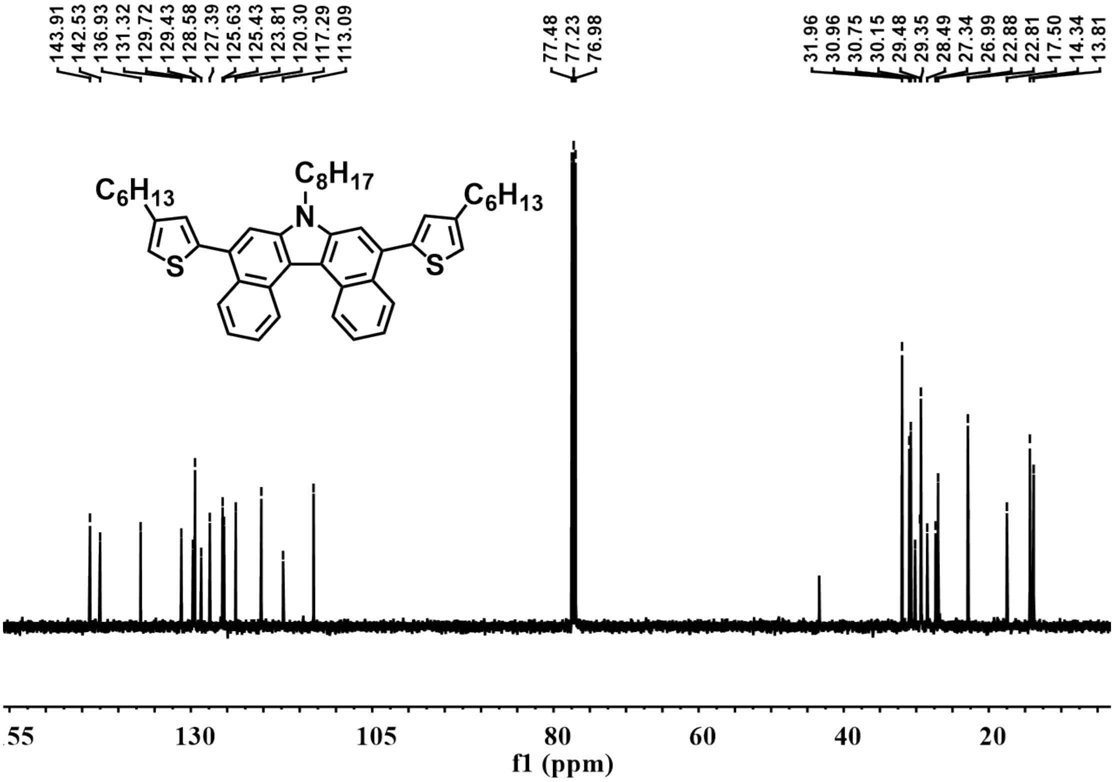

Fig. S12 ^{13}C NMR spectrum of **Compound 3**.

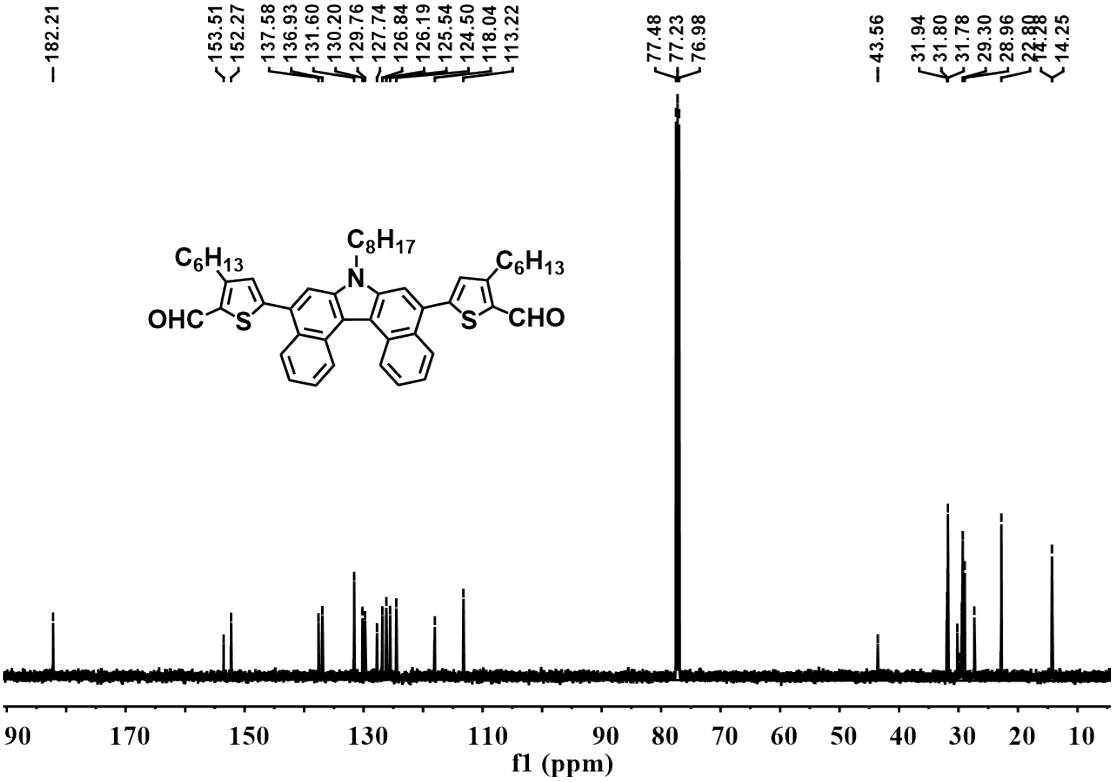

Fig. S13 ^{13}C NMR spectrum of **Compound 4**.

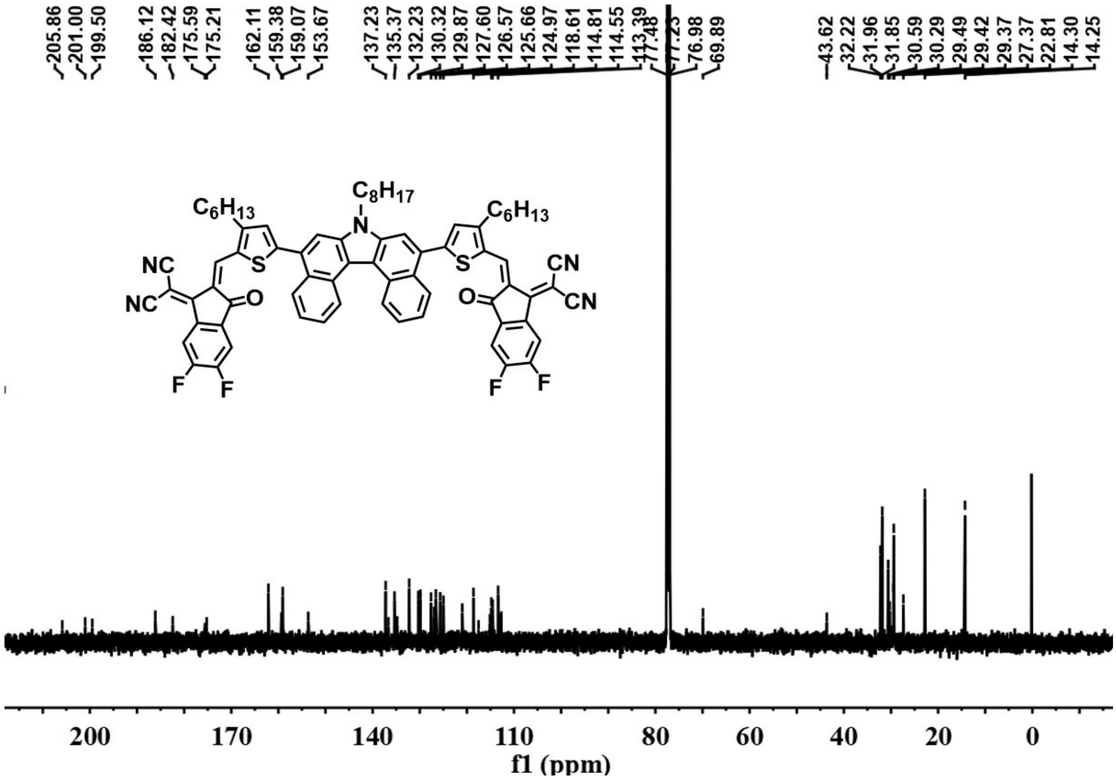

Fig. S14 ^{13}C NMR spectrum of **DCB-4F**.

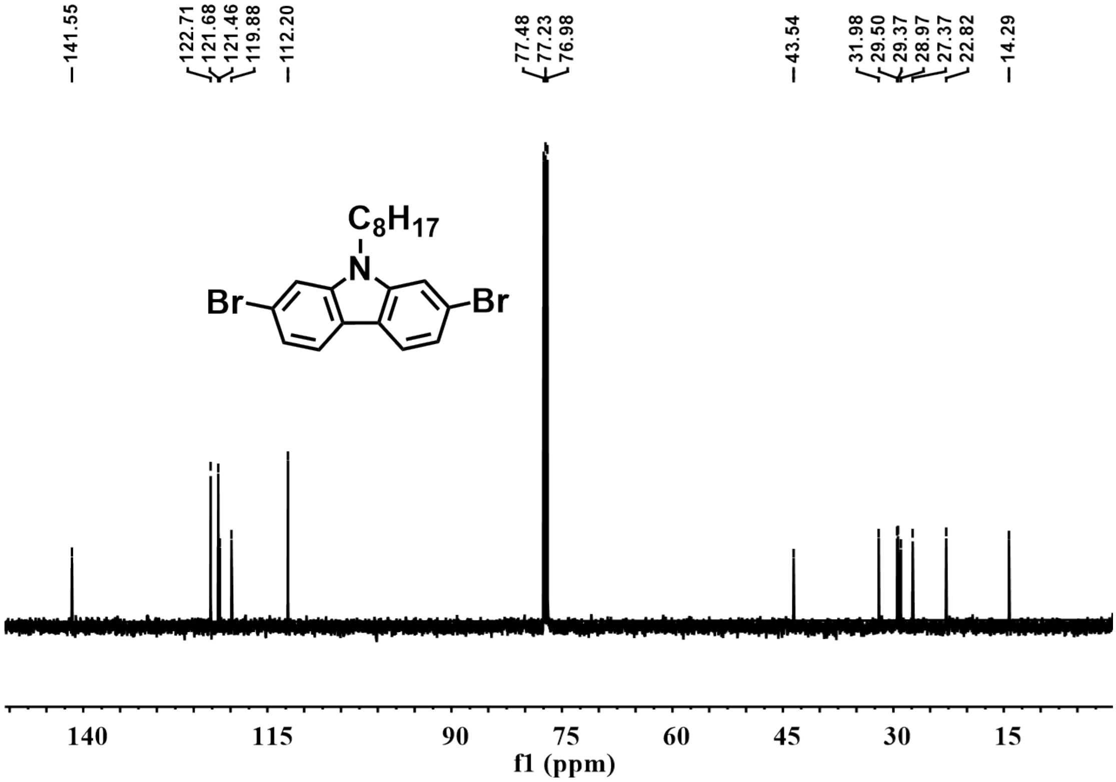

Fig. S15 ^{13}C NMR spectrum of **Compound 5**.

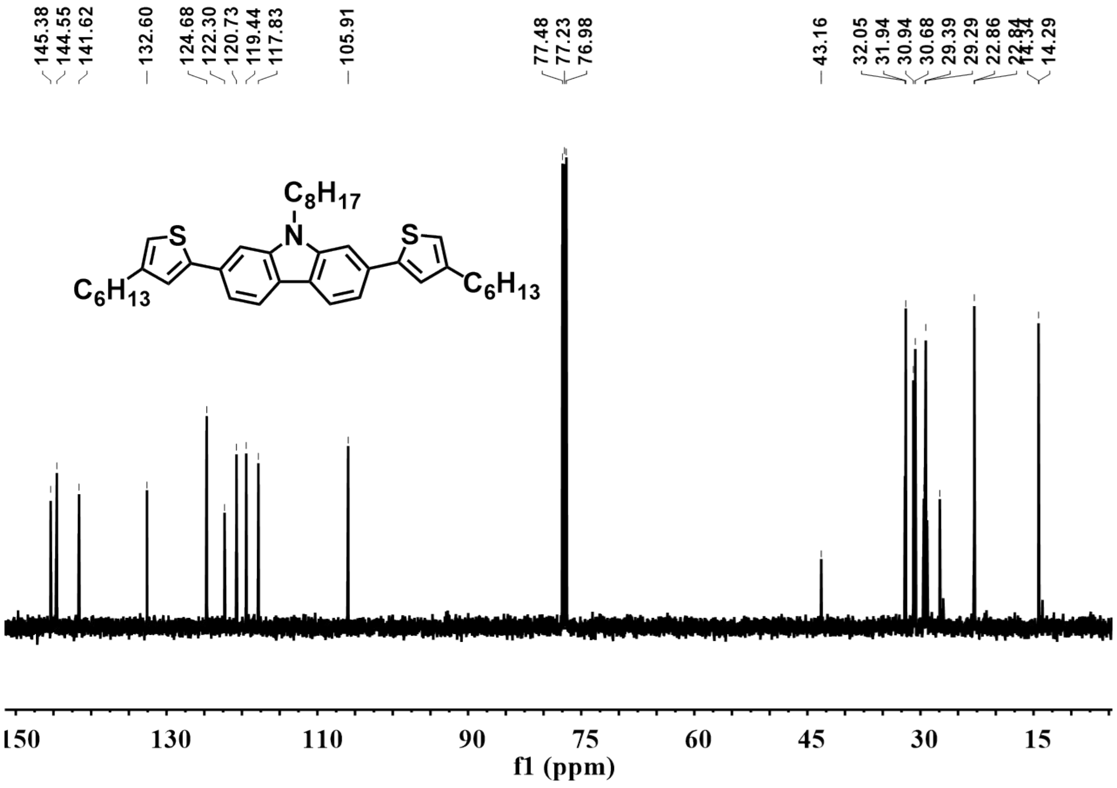

Fig. S16 ^{13}C NMR spectrum of **Compound 6**.

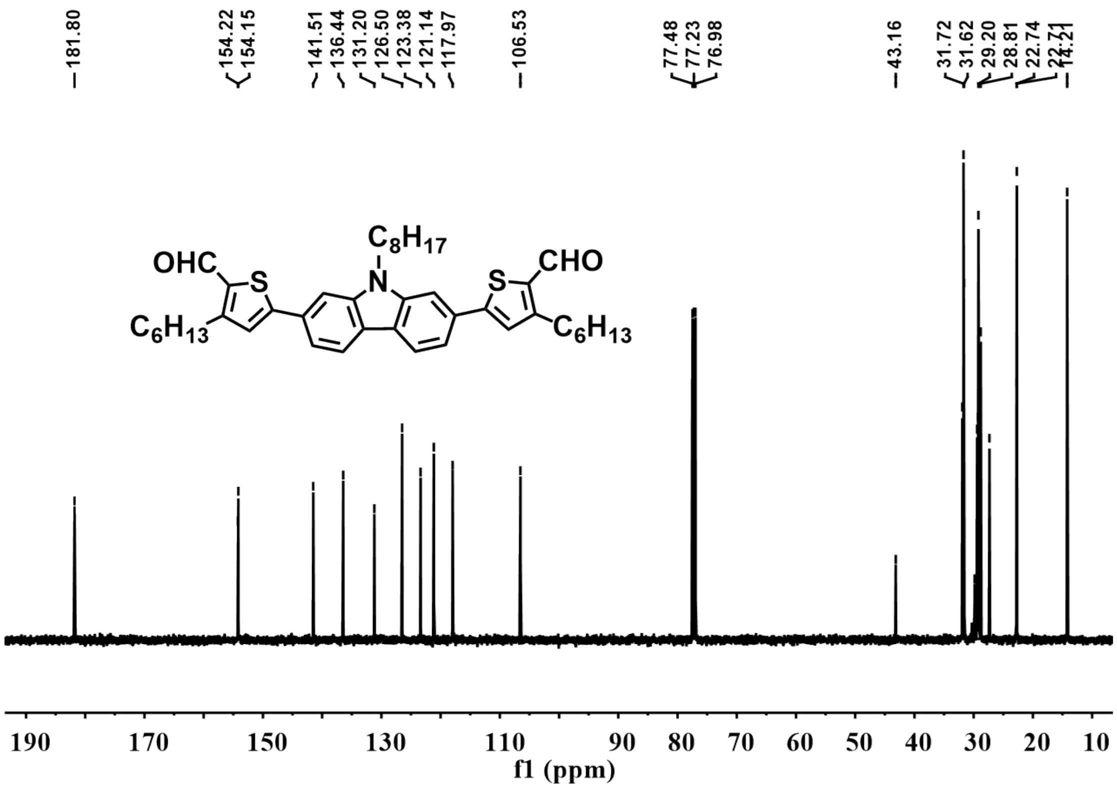

Fig. S17 ^{13}C NMR spectrum of **Compound 7**.

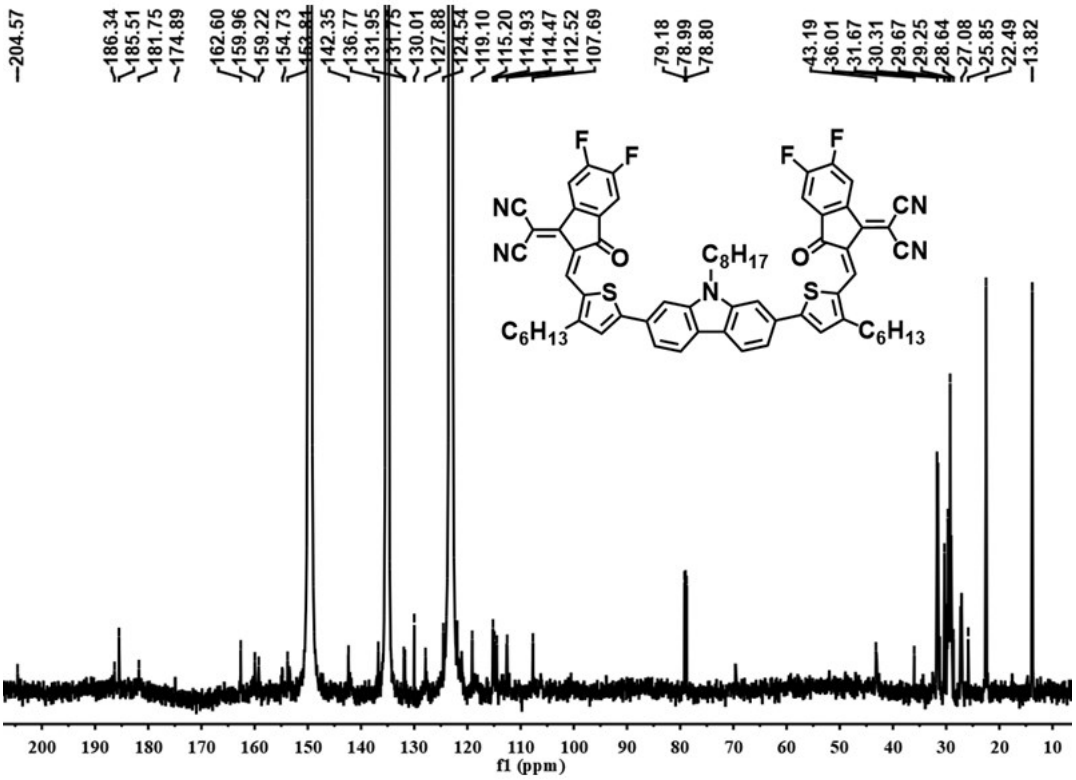

Fig. S18 ^{13}C NMR spectrum of **CB-4F** (from Bruker AVANCE NEO 700 MHz).

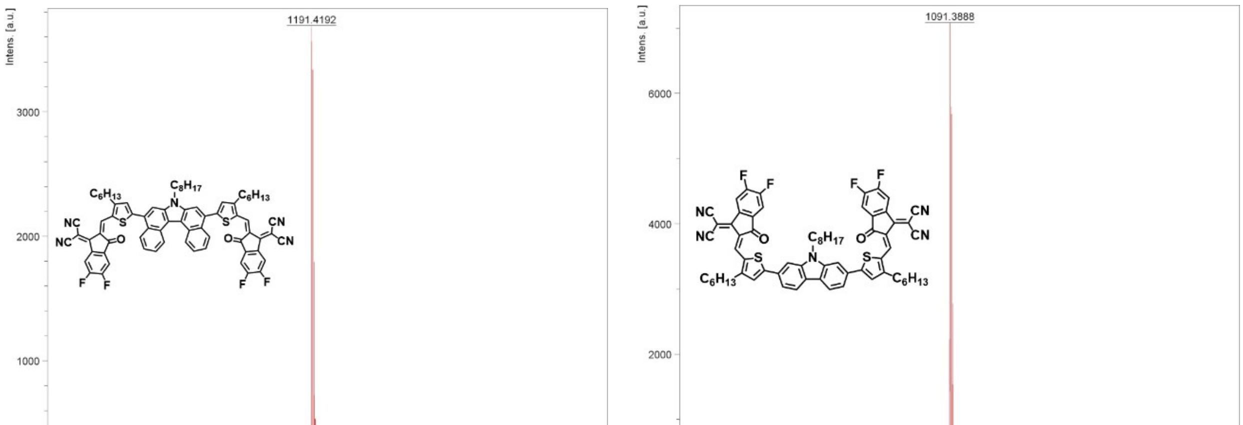

Fig. S19 The MALDI-TOF MS plots of **DCB-4F** and **CB-4F.**

4. TGA analysis

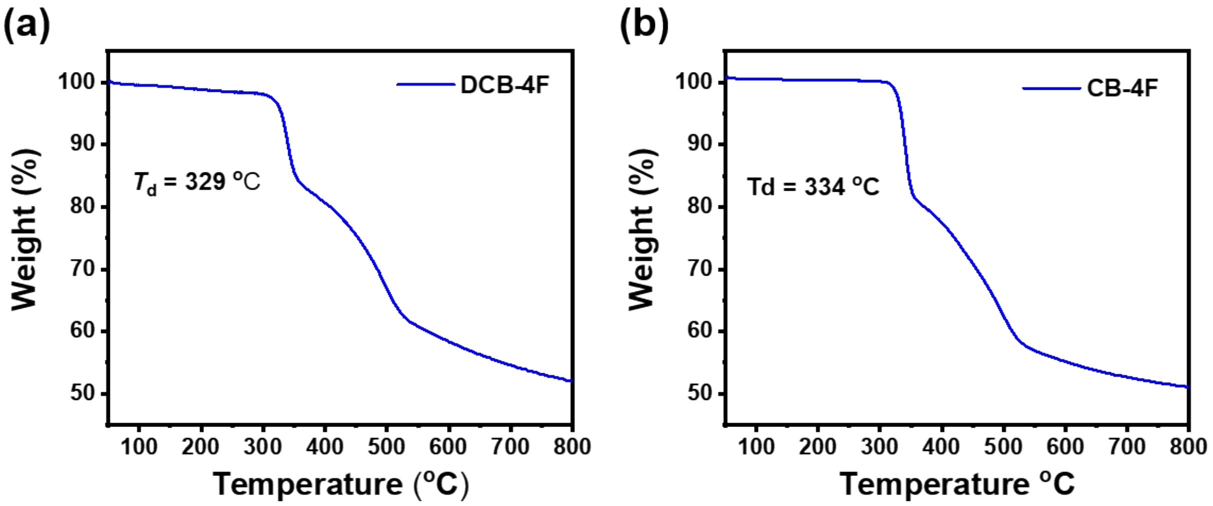

Fig. S20 TGA measurements of (a) DCB-4F and (b) CB-4F with a ramping rate of 20 °C/min.

5. Calculation of CB-4F

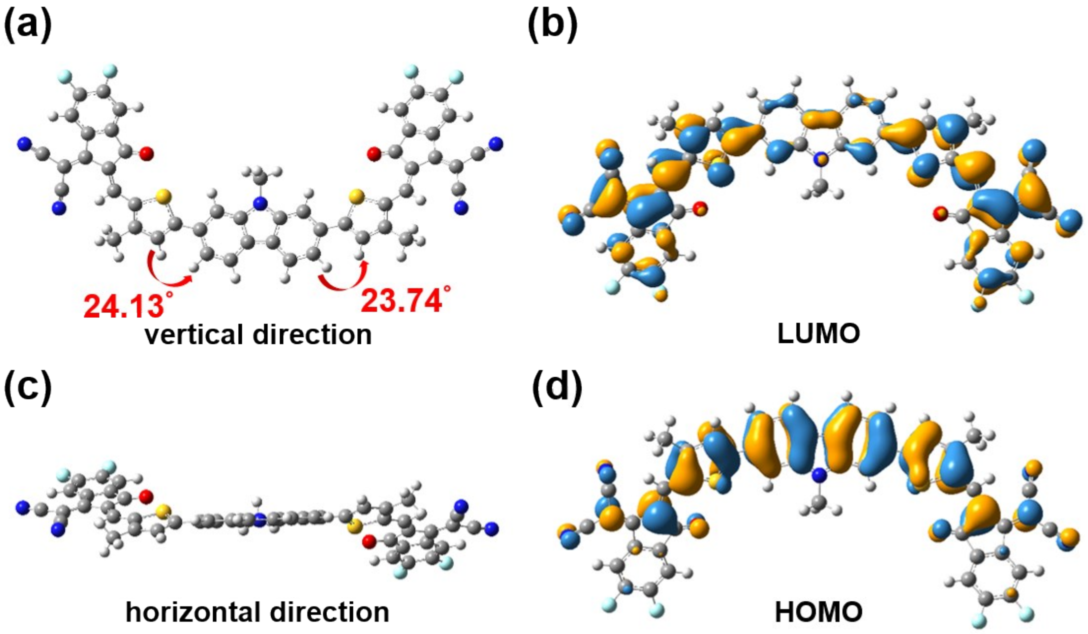

Fig. S21 Molecular conformations and frontier orbitals of CB-4F calculated by DFT.

6. OSCs chacterization

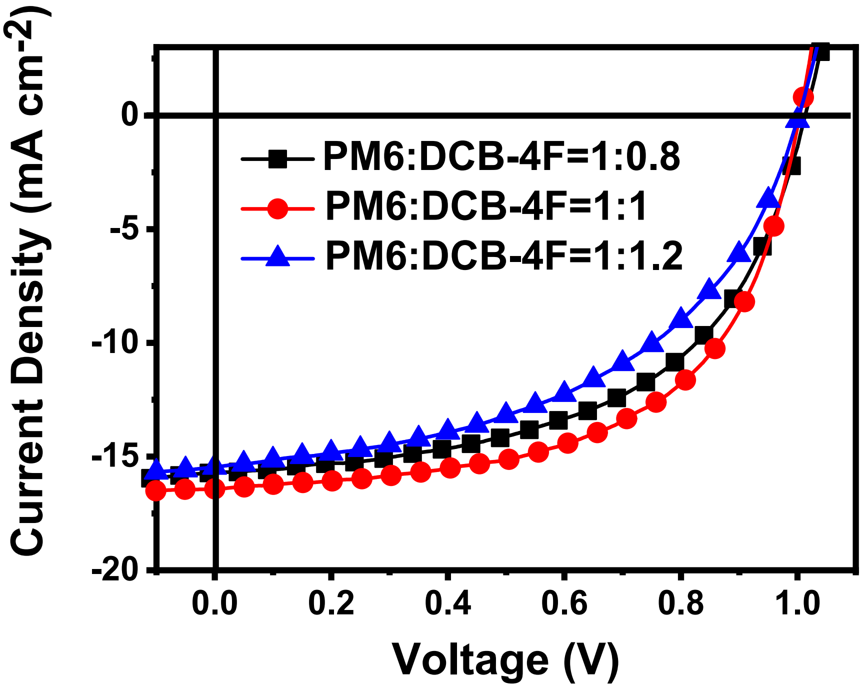

Fig. S22 *J-V* curves of the PM6:DCB-4F based devices with different D/A ratios.

Table S2. Optimization process of the PM6:DCB-4F as-cast devices.

PM6:DCB-4F	V_{OC} [a] (V)	J_{SC} [a] (mA cm^{-2})	FF [a] (%)	PCE [a] (%)
1:0.8	1.01 (1.01±0.01)	15.71 (15.16±0.52)	54.76 (54.12±0.61)	8.69 (8.51±0.14)
1:1	1.00 (1.00±0.01)	16.42 (15.96±0.43)	58.23 (57.65±0.57)	9.56 (9.46±0.08)
1:1.2	1.00 (1.00±0.01)	15.47 (14.97±0.48)	49.35 (48.87±0.46)	7.63 (7.51±0.11)

[a] Statistical results are obtained from over 12 devices and listed in parentheses.

Table S3. The optimized photovoltaic parameters of PM6:DCB-4F (1:1) devices with different additives

Additive	V_{OC} (V) [a]	J_{SC} (mA cm^{-2}) [a]	FF (%)[a]	PCE (%)[a]
none	1.00 (1.00±0.01)	16.42 (15.96±0.43)	58.23 (57.65±0.57)	9.56 (9.46±0.08)
0.5% DIO	**1.00** **(1.00±0.01)**	**17.28** **(16.69±0.56)**	**62.52** **(61.89±0.60)**	**10.80** **(10.52±0.24)**

1.0% DIO	0.96 (0.95±0.01)	10.80 (10.31±0.47)	60.19 (59.72±0.43)	6.24 (6.07±0.15)
0.5% CN	1.00 (1.01±0.01)	15.21 (14.86±0.34)	62.46 (61.88±0.55)	9.50 (9.39±0.09)

[a] The average values were obtained from over 12 devices.

Table S4. The photovoltaic parameters of 0.5 vol% DIO processed PM6:DCB-4F (1:1) devices at different thermal annealing temperature (TAT) for 10 min

TAT (℃)	**V_{OC} (V) [a]**	**J_{SC} (mA cm^{-2}) [a]**	**FF (%)[a]**	**PCE (%)[a]**
none	1.00 (1.00±0.01)	17.28 (16.69±0.56)	62.52 (61.89±0.60)	10.80 (10.52±0.24)
80	0.95 (0.96±0.01)	16.42 (16.01±0.39)	70.35 (69.90±0.42)	10.97 (10.81±0.14)
100	**0.94** **(0.95±0.01)**	**16.66** **(16.09±0.43)**	**70.79** **(70.07±0.68)**	**11.08** **(10.83±0.19)**
120	0.94 (0.93±0.01)	15.47 (14.97±0.48)	70.54 (69.93±0.57)	10.26 (10.06±0.18)

[a] The average values were obtained from over 12 devices.

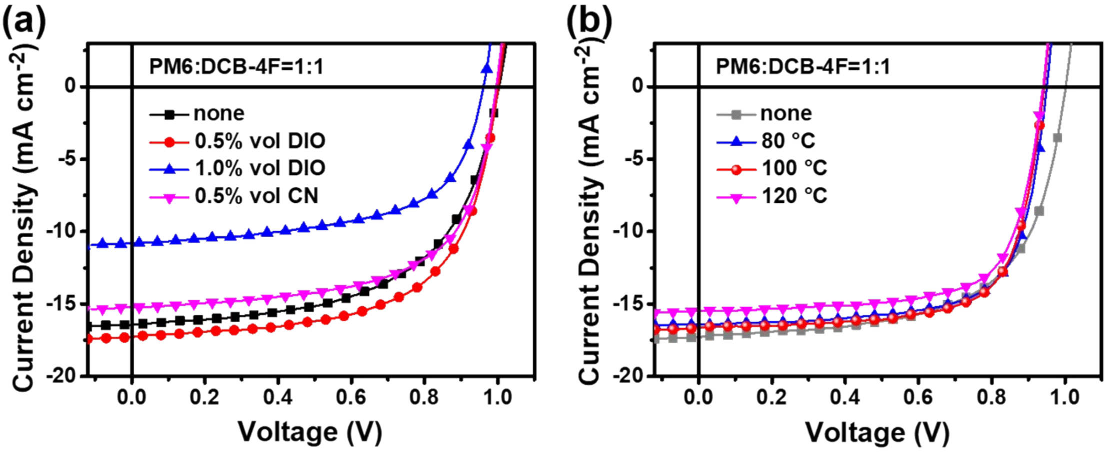

Fig. S23 *J-V* curves of PM6:DCB-4F (1:1) devices (a) with different additive and (b) at different thermal annealing temperature with 0.5 vol% DIO as processing additive.

Table S5. Device photovoltaic parameters of PM6:DCB-4F:PC$_{71}$BM as-cast OSCs

PM6:DCB-4F:PC$_{71}$BM	V_{OC} [a] (V)	J_{SC} [a] (mA cm^{-2})	J_{cacl} [b] (mA cm^{-2})	FF [a] (%)	PCE [a] (%)

1:1:0	1.00 (1.01±0.01)	16.42 (15.96±0.43)	15.75	58.23 (57.65±0.57)	9.56 (9.46±0.08)
1:1:0.1	1.00 (1.00±0.01)	16.79 (16.19±0.58)	16.09	66.53 (65.83±0.64)	11.17 (11.06±0.06)
1:1:0.2	0.99 (1.00±0.01)	16.51 (16.02±0.39)	15.83	63.91 (63.27±0.61)	10.45 (10.27±0.15)

[a] Statistical results obtained from over 12 devices and listed in parentheses. [b] Calculated J_{SC} values integrated from external quantum efficiency (EQE) spectra.

7. SCLC mobility, Voc vs. light intensity and contact angle measurement

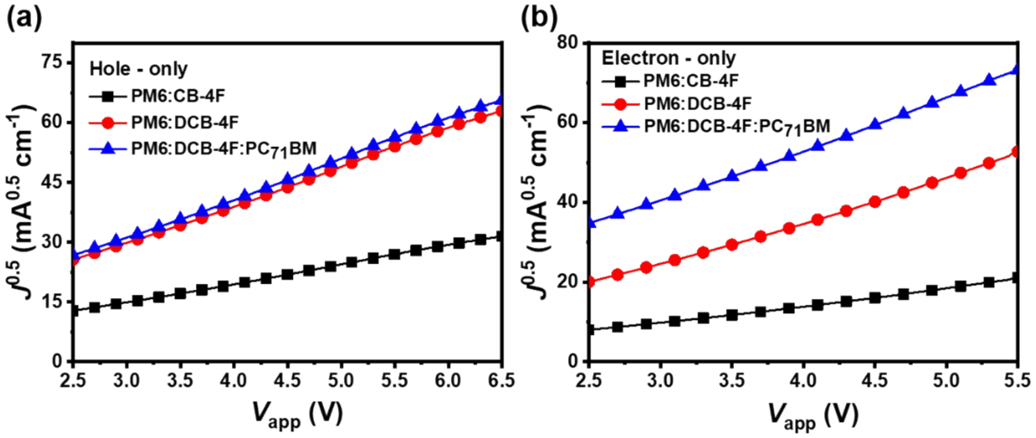

Fig. S24 $J^{0.5}$-V characteristics were acquired from (a) hole-only and (b) electron-only devices based on PM6:CB-4F, PM6:DCB-4F and PM6:DCB-4F:$PC_{71}BM$.

Table S6. Electron and hole mobilities of the optimized PM6:DCB-4F and PM6:CB-4F as-cast devices.

Blend Film	μ_h (cm^2 V^{-1} s^{-1})	μ_e (cm^2 V^{-1} s^{-1})	μ_h/μ_e
PM6:DCB-4F (1:1)	3.75×10^{-4}	1.33×10^{-4}	2.82
PM6:CB-4F (1:1)	1.64×10^{-4}	0.32×10^{-4}	4.56
PM6:DCB-4F:$PC_{71}BM$ (1:1:0.1)	3.91×10^{-4}	2.56×10^{-4}	1.53

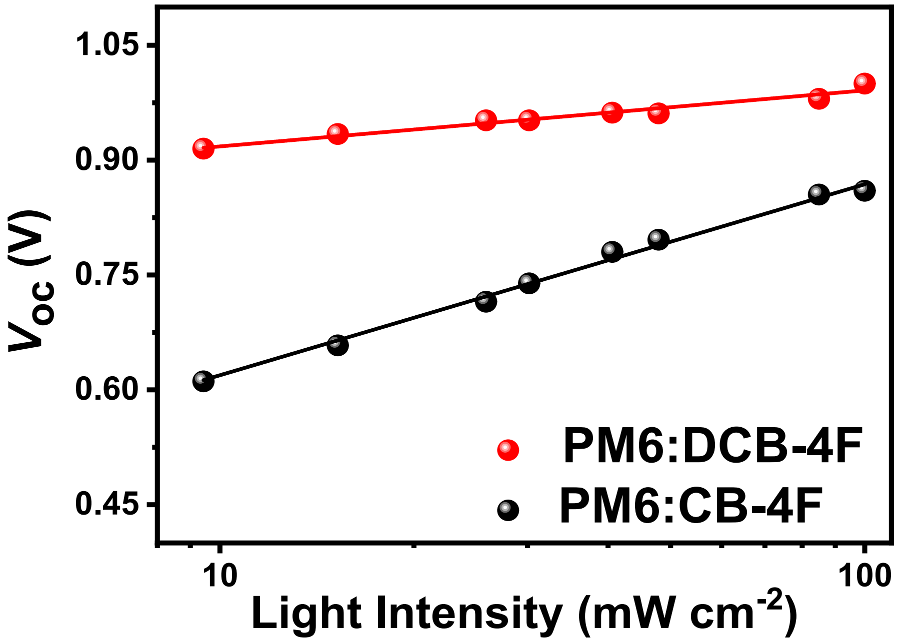

Fig. S25 Light intensity dependence of V_{OC} of the optimized PM6:DCB-4F and PM6:CB-4F based devices.

Table S7. Surface tension and interaction parameters of PM6 and acceptors.

Pure Film	θ_{water} (deg)	θ_{GL} (deg)	γ (mN m^{-1})	Blend Film	χ
PM6	98.0	93.1	20.21	---	---
DCB-4F	78.9	64.9	35.07	PM6:DCB-4F	2.0347
CB-4F	59.9	22.8	61.13	PM6:CB-4F	11.0424

Reference

1. L. Zhan, S. Li, S. Zhang, X. Chen, T. K. Lau, X. Lu, M. Shi, C. Z. Li and H. Chen, *ACS Appl. Mater. Interfaces*, 2018, **10**, 42444-42452.
2. Y. Wang, Z. Liu, X. Cui, C. Wang, H. Lu, Y. Liu, Z. Fei, Z. Ma and Z. Bo, *J. Mater. Chem. A*, 2020, **8**, 12495-12501.
3. S. Li, L. Zhan, F. Liu, J. Ren, M. Shi, C. Z. Li, T. P. Russell and H. Chen, *Adv. Mater.*, 2018, **30**, 1705208.

4. Y.-Q.-Q. Yi, H. Feng, N. Zheng, X. Ke, B. Kan, M. Chang, Z. Xie, X. Wan, C. Li and Y. Chen, *Chem. Mater.*, 2019, **31**, 904-911.
5. J. Lee, S.-J. Ko, H. Lee, J. Huang, Z. Zhu, M. Seifrid, J. Vollbrecht, V. V. Brus, A. Karki, H. Wang, K. Cho, T.-Q. Nguyen and G. C. Bazan, *ACS Energy Lett.*, 2019, **4**, 1401-1409.
6. S. Li, L. Zhan, T. K. Lau, Z. P. Yu, W. Yang, T. R. Andersen, Z. Fu, C. Z. Li, X. Lu, M. Shi and H. Chen, *Small Methods*, 2019, **3**, 1099531.
7. Z. P. Yu, Z. X. Liu, F. X. Chen, R. Qin, T. K. Lau, J. L. Yin, X. Kong, X. Lu, M. Shi, C. Z. Li and H. Chen, *Nat. Commun.*, 2019, **10**, 2152.
8. R. Zheng, Q. Guo, D. Hao, C. Zhang, W. Xue, H. Huang, C. Li, W. Ma and Z. Bo, *J. Mater. Chem. C*, 2019, **7**, 15141-15147.
9. X. Li, Z. Xu, X. Guo, Q. Fan, M. Zhang and Y. Li, *Org. Electron.*, 2018, **58**, 133-138.
10. H. Huang, Q. Guo, S. Feng, C. Zhang, Z. Bi, W. Xue, J. Yang, J. Song, C. Li, X. Xu, Z. Tang, W. Ma and Z. Bo, *Nat. Commun.*, 2019, **10**, 3038.